A Focused Super-Continuum Solar Simulator for Illuminated Solar Cell Microscopy

T. Dennis

National Institute of Standards and Technology
325 Broadway, Boulder, CO, USA, tasshi@nist.gov

ABSTRACT

The design and application of a novel, focused solar simulator based on a high-power, super-continuum laser is described in this work. The simulator light was focused to a spot approximately 8 µm in diameter, and used to create micrometer-scale spatial maps of full-spectrum, optical-beam-induced current in sample solar cells. Microscopic details such as grid lines, damage spots, and material variations were selectively excited and spatially resolved on GaAs and CIGS thin film cells. The simulator features continuous spectral coverage from the visible to the infrared, and the ability to be arbitrarily spectrally shaped. The partial currents generated by a GaAs cell from spectrally sliced illumination were shown to be consistent with the external quantum efficiency of such a device. With refinements to the focusing optics, it is anticipated that this unique tool can be effectively used to characterize the detailed operation of solar-cell materials and devices at the nano-scale.

Keywords: microscopy, multi-junction, obic, solar simulator, super-continuum

1 INTRODUCTION

Further improvements to solar cell efficiency for all materials and technologies depend critically on a better understanding of their optical and electrical characteristics at the micrometer and nanometer scale. The study of defects caused by impurities or crystalline grain boundaries, artifacts and edge effects from deposition processes, and third-generation materials having micro-arrays or structured conduction paths, could all potentially benefit from the ability to selectively excite material features with a diffraction-limited focus. In addition, the characterization of multi-junction materials could benefit from independent excitation of the different junctions made possible by spectral shaping [1]. Traditional solar simulators are based on lamps, such as the xenon arc-lamp [2], or arrays of light-emitting diodes [3]. However, it is challenging to efficiently apply these light sources to measurement systems that require focused and/or spectrally shaped light. Fundamentally, bulb-based and point light sources typically radiate into large solid angles, thereby generating a low number of photons for any single spatial mode. This low spatial coherence makes it difficult if not impossible to efficiently use optical beam processing to achieve diffraction-limited focusing and/or arbitrary spectral shaping.

Recently, high-power super-continuum lasers that offer spectral coverage from the visible (blue) out to the infrared have become commercially available. These fiber-based, white-light lasers generate watts of optical power in a single spatial mode across the entire spectrum, enabling diffraction-limited beam propagation. Previously, we demonstrated that various sample solar cell materials responded to this novel light source as if it were a traditional, lamp-based simulator [4].

In this work, we report on the application of our novel solar simulator to the microscopic excitation of photocurrent in sample solar cells. The focusing of the simulator output is quantified, and spatial maps of full-spectrum optical-beam-induced current (FS-OBIC) from sample materials are presented and compared to optical microscopy. Also, the ability to arbitrarily spectrally shape the simulator is demonstrated and used to generate partial currents in a GaAs solar cell.

2 SIMULATOR DESIGN AND FOCUSING

The design and construction of our simulator has been described previously [4], and utilizes a commercially available super-continuum laser having more than 8 W of emission and a spectrum that spans from below 450 nm to beyond 2200 nm. We operate this pulsed laser source (400 fs pulses) at its maximum repetition rate of 80 MHz to achieve the broadest spectrum with the most content at short wavelengths. Figure 1 illustrates our approach for

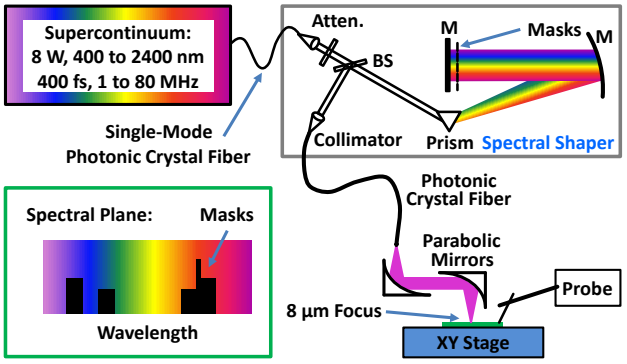

Figure 1: The focused solar simulator system, including mask geometry (green box). M: mirror; BS: beamsplitter

CTSI-Cleantech 2013, www.ct-si.org, ISBN 978-1-4822-0594-7

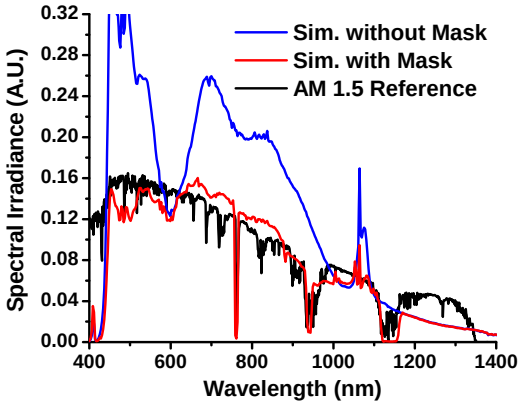

Figure 2: Simulator spectra with the amplitude mask of the spectral shaper (red curve) and without (blue curve). The AM 1.5 reference spectrum (black curve) is shown for comparison.

spectrally shaping the source by use of a dispersive spectrometer. A prism of F2 glass was used to spread the beam across a collimation mirror having a focal length of 500 mm. The spectral beam was then directed onto a planar mirror located at the focal point of the collimation mirror to achieve maximum spectral resolution. Not shown in Fig. 1 is a cylindrical lens before the prism, which was used to expand the beam out of the plane of the page. In contrast to a line focus, this expanded beam in the spectral plane allowed varying amounts of light to be attenuated at any given wavelength by static amplitude masks. The planar mirror then returned the light back to the prism, where it was recombined into an 8 mm diameter spatial beam and focused into a photonic crystal fiber.

Presented in Fig. 2 is the output spectrum of the shaper propagating in the photonic crystal fiber with (red curve) and without (blue curve) an amplitude mask, along with the AM 1.5 (ASTM G-173-03) solar reference spectrum as the black curve [5]. A fairly good spectral match to the reference is achieved, with simulation of selected water absorption features. With additional effort, the amplitude mask could be refined to achieve an even better spectral match. We also applied additional masks to slice the simulator spectrum into sub-bands. Fig. 3 presents

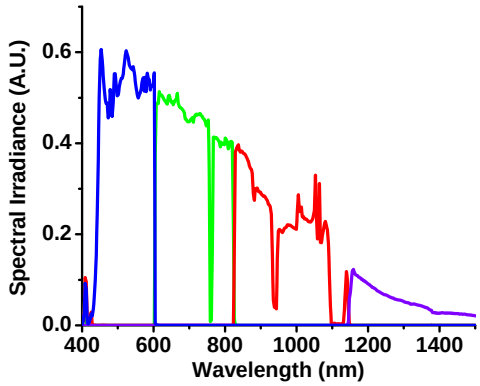

Figure 3: Measured spectra are shown for the selective excitation of multi-junction cell layers.

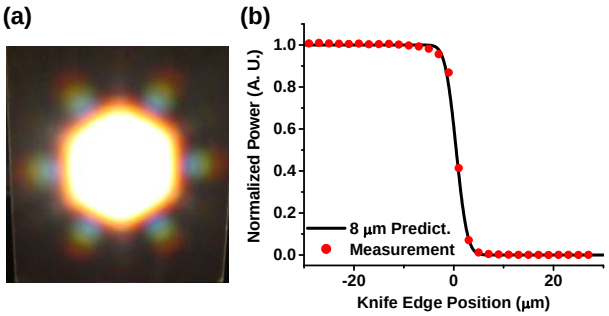

Figure 4: (a) The projected light distribution emitted from the simulator output fiber and (b) the knife-edge measurement of the focused spot.

measurements of four different spectra created for the excitation of individual layers in a 4-junction solar cell.

Figure 4(a) shows the projected spatial pattern of the broadband light diverging from the photonic crystal output fiber of the spectral shaper. The large central lobe represents broadband propagation of light within the 8 µm glass core of the fiber. Surrounding this are six smaller lobes that represent propagation in the hexagonal array of air holes encircling the glass core. While the spatial distribution in Fig. 4(a) does not have a traditional Gaussian profile, it is clear that the majority of the light propagates in the central lobe. The broadband single-mode characteristic of the photonic crystal fiber is critical to achieving a focus that is diffraction limited.

The diverging light from the photonic crystal output fiber was collimated and focused by aluminum parabolic mirrors having focal lengths of approximately 50 mm and 20 mm, respectively. We used a scanning, knife-edge technique to estimate the diameter of the focused spot to be about 8 µm, which for a Gaussian beam profile would contain 86 % of the beam power. The knife-edge measurement is presented in Fig. 4(b), and illustrates that the slope of the transmitted power through the central lobe (zero position) compares well to the prediction for an 8 µm Gaussian beam. A small deviation is apparent at the upper knee that may be consistent with the side-lobe distribution.

3 FULL SPECTRUM MEASUREMENTS

The short-circuit current induced by the focused simulator was spatially mapped across sample solar cells by use of a raster scanning system that translated the sample. In these FS-OBIC measurements, the irradiance of the focused spot was approximately equivalent to 160 suns. Figure 5 shows the measured current map of an n-GAInP/p-GaAs heterojunction concentrator cell provided by the National Renewable Energy Laboratory (NREL). In this 500 µm x 500 µm image made with 10 µm translation steps, the depressed dark regions were created by metallic grid lines on the cell, which shadowed the active material. The production of current from the active regions of the cell

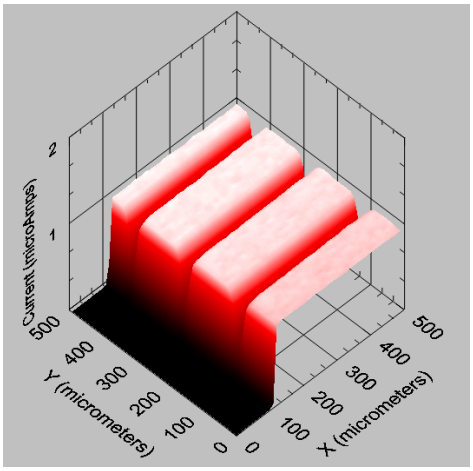

Figure 5: The current map of a GaAs solar cell with grid lines.

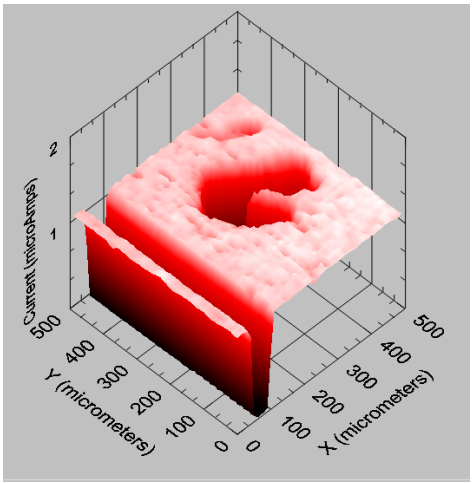

Figure 6: The current map of a CIGS cell featuring a grid line, damage spot, and surface variations.

is indicated by the light-colored mesa structures and is about 1 µA. The highly uniform current map is consistent with the high efficiency of the device (measured to be 15.2 % by NREL) and the crystalline composition.

Figure 6 presents the results of an FS-OBIC measurement on a copper indium gallium selenide (CIGS) thin film solar cell, also from NREL. The long trench feature was caused by a grid line, and the induced current in the active regions was a little over 1 µA. The central crater was caused by a small scratch in the film intentionally created with a pin point, and indicates the localized impact on the production of photocurrent. The active area of the CIGS cell shows a distinct spatial variation or roughness. Typical of this CIGS material, grain structures of just a few micrometers in size arranged in clusters of 10 µm or more are expected.

Figure 7(a) is a top view of Fig. 6, to enable side-by-side comparison with the optical-microscopy image of the CIGS cell shown in Fig. 7(b). It is clear from the optical

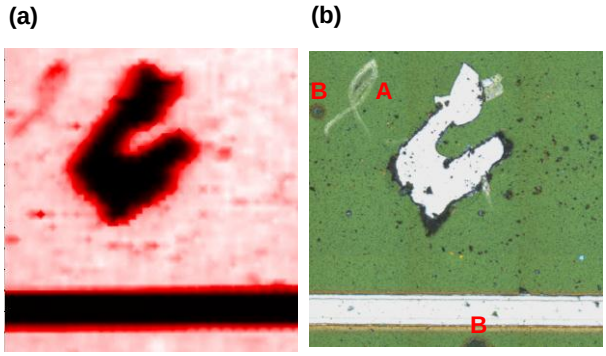

Figure 7: (a) Top-view map of the CIGS cell (Fig. 6) with (b) an optical microscopy image of the region.

microscopy that the pin-point scratch caused complete removal of the thin film from the glass substrate. By contrast, the smaller ribbon-like feature in the upper left corner (labeled with "A") may only be partial film damage, causing a slight reduction (darkening) in the current map. The small, dark, speckle features across Fig. 7(b) would appear to be film debris from creating the scratch. Some of their locations correlate with reductions in current. Two more features of interest in Fig. 7(b) are a brown spot found to the left of the ribbon-like feature and another brown spot partially shown at the bottom center of the image (both labeled with "B"). In the upper left instance, the feature corresponds to a reduction in current (dark spot), while the lower one appears to generate increased current (white spot). A topographic image of this area of the cell indicated that these brown spots reside in the volume of the film, whereas the small, speckle features rest on top.

4 SLICED SPECTRUM MEASUREMENTS

To develop the multi-junction measurement capabilities of the focused simulator, we characterized the partial currents generated by a single-junction cell from spectrally sliced illumination. Fig. 8 shows two sliced spectra created by the simulator, which we have colored and labeled as the blue and red spectra. The spectra were sliced at a wavelength of 720 nm so as to have nearly equal total power within the wavelength range shown. Also shown in the figure is the external quantum efficiency (EQE) of a GaAs solar cell from NREL that is very similar to the device used throughout this work [6]. While not the actual EQE of our device, the curve should be sufficient to estimate the measured partial currents when used in conjunction with the measured spectra.

Figure 9(a) shows a full-spectrum OBIC measurement of the GaAs cell with a focused spot irradiance that was approximately equivalent to 50 suns. Figures 9(b) and 9(c) show the OBIC measurements for spectrally sliced blue and red illumination, respectively. The average currents measured in the middle of the active regions were 0.115 µA for the blue illumination and 0.055 µA for the red illumination. The sum of these currents agrees well with the

CTSI-Cleantech 2013, www.ct-si.org, ISBN 978-1-4822-0594-7

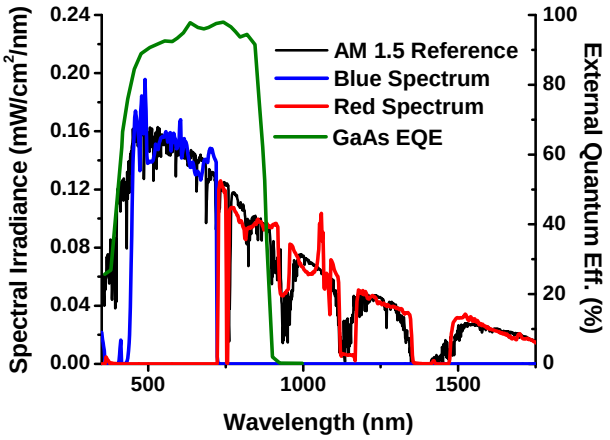

Figure 8: Sliced spectra for inducing partial currents are shown with the external quantum efficiency (EQE) of a representative GaAs single-junction cell.

0.174 µA current measured for full-spectrum illumination in Fig. 9(a).

By using the curves of Fig. 8, we estimated that 73 % of the total current should be produced from blue light illumination, whereas the remaining 27 % should be produced from red light illumination. Because the EQE for this device rolls off substantially above 850 nm, more current is expected from blue illumination despite the nearly equal powers delivered to the device. Comparing the currents of Fig. 9, we measured 68 % of the current from blue illumination and 32 % from red illumination. The agreement is quite good, keeping in mind that the actual EQE curve for the device was not available.

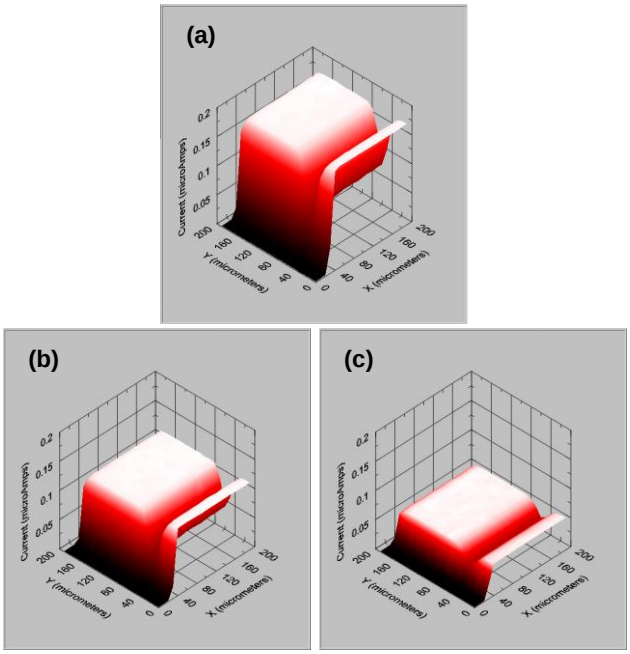

Figure 9: Current maps for (a) full-spectrum illumination, (b) blue light illumination, and (c) red light illumination of a GaAs solar cell.

5 DISCUSSION AND CONCLUSION

With better utilization of our optics, we anticipate achieving a much smaller focused spot. An approximate expression for the spot size diameter of a focused Gaussian beam at wavelength λ by an objective with f-number $f^{\#}$ is given by $2\lambda f^{\#}$. The f-number of our focusing parabolic mirror was 0.5, which indicates that by using the full numerial aperature we could achieve a spot equal to the wavelength of the light. For our broadband simulator the spot size has a wavelength dependence, although some of this depedence may be compensated by the spatial distribution of the light being focused (see Fig. 4(a)). While further study is required, a smaller spot would enable the illumination of individual grains in thin films and engineered nanostructured materials.

Our focused solar simulator has shown the ability to selectively excite micrometer-scale features in advanced photovoltaic materials with spectrally shaped light. A full-spectrum, focused spot 8 µm in diameter was used to study current variations in FS-OBIC spatial maps of sample solar cells. The spectrally selective generation of current in a single junction was also demonstrated, and will be extended in future work to imaging of multi-junction devices.

The author gratefully acknowledges A. Sanders of NIST for optical and topographic microscopy, K. Bertness of NIST for useful technical discussions, and D. Friedman and L. Mansfield of NREL for providing the sample cells.

REFERENCES

[1] T. Moriarty, J. Jablonski, and K. Emery, "Algorithm for Building a Simulator Spectrum for NREL One-Sun Multi-Source Simulator," Thirty-eighth PVSC, 1291-1295, 2012.

[2] K. Emery, D. Myers, and S. Rummel, "Solar Simulation – Problems and Solutions", Twentieth PVSC, 1087-1091, 1988.

[3] Y. Tsuno, K. Kamisako, and K. Kurokawa, "New Generation of PV Module Rating by LED Solar Simulator – A Novel Approach and its Capabilities," Thirty-third PVSC, 1-5, 2008.

[4] T. Dennis, J. B. Schlager, H.-C. Yuan, Q. Wang, and D. Friedman, "A Novel Solar Simulator Based on a Super-Continuum Laser," Thirty-eighth PVSC, 1845-1848, 2012.

[5] G173003(2008) Standard Tables for Reference Solar Spectral Irradiances: Direct Normal and Hemispherical on 37º Tilted Surfaces, available at http://astm.org.

[6] S. R. Kurtz, J. M. Olson, and A. Kibbler, "High Efficiency GaAs Solar Cells Using GaInP2 Window Layers," Twenty-first PVSC, 138-140, 1990.